

# Extracting many-particle entanglement entropy from observables using supervised machine learning

Richard Berkovits

*Department of Physics, Jack and Pearl Resnick Institute, Bar-Ilan University, Ramat-Gan 52900, Israel*

Entanglement, which quantifies non-local correlations in quantum mechanics, is the fascinating concept behind much of aspiration towards quantum technologies. Nevertheless, directly measuring the entanglement of a many-particle system is very challenging. Here we show that via supervised machine learning using a convolutional neural network, we can infer the entanglement from a measurable observable for a disordered interacting quantum many-particle system. Several structures of neural networks were tested and a convolutional neural network akin to structures used for image and speech recognition performed the best. After training on a set of 500 realizations of disorder, the network was applied to 200 new realizations and its results for the entanglement entropy were compared to a direct computation of the entanglement entropy. Excellent agreement was found, except for several rare region which in a previous study were identified as belonging to an inclusion of a Griffiths-like quantum phase. Training the network on a test set with different parameters (in the same phase) also works quite well.

Recently there has been a growing interest in understanding quantum entanglement [1–5]. The concept of entanglement lies at the heart of quantum mechanics [6] and its application in the emerging field of quantum technologies [7].

In many-particle systems, entanglement is traditionally quantified by the entanglement entropy [1–5], i.e., the measure of the amount of information in the reduced density matrix of part of the system when the degrees of freedom of the remainder of the system are traced out. This entanglement entropy is used e.g. to identify phases of many-body systems such as insulator or metallic phases [8–11], or topological phases [12–14].

Nevertheless, in contrast to few-particle systems, measurement of entanglement for many-particle systems turns out to be very challenging. Despite the growing importance of entanglement in theoretical physics, current condensed matter experiments do not have a direct probe with which to measure entanglement. One can quantify the entanglement through the measurement of the second Rényi entropy, which measures the overlap between the ground state of two identical copies of a system when a region is swapped between them [15, 16]. It was realized that this could be actually measured through coupling between two identical copies of cold atom systems [17, 18]. This measurement has indeed been performed on such systems [19, 20]. Another way, which has recently been proposed [21], involves repeatedly applying time dependent disorder potentials and projective measurement. After statistical analysis, the second Rényi entropy may be extracted. This method avoids the need for cloning copies of the system, which is difficult even for cold atom systems and impossible for condensed matter systems, nonetheless, applying this method raises its own set of challenges.

Here, a different tack on extracting the entanglement entropy of a region in a many-particle system is taken. The method is based on utilizing the apparent correlation

between the variance of the number of particles in the sub-system and the entanglement entropy. A connection between the summation of a weighted series of cumulants of the number of particles in the sub-system and the entanglement entropy was established by Klich and Levitov [22, 23] for non-interacting free fermions. This theory was extended to include disordered systems by Burmistrov *et al.* [24]. These relations are no longer exact for interacting fermions [25]. Nevertheless, since here interactions do not change the phase of the system which remains an Anderson insulator, and by looking at the number variance vs. the entanglement entropy (see Fig. 1), it is clear that even for disordered interacting systems there is a strong correlation between the two quantities. This indicates that within the chaotic-like data of the particle variance data on the entanglement is embedded. Since experimentally the variance in the number of particles is accessible and the entanglement entropy is not, and for many numerical procedures it is computationally simpler to calculate the number of particles in a sub-region than the entanglement of that region, it would be very useful to extract one from the other. In order to do so, machine learning will be utilized in order to train a convolution neural network (the term will be explained later) on a finite number of realizations of disorder and evaluate its performance on a different set of realizations. It will be shown that after such training, the neural network is able to map the number variance to the entanglement entropy of a given realization with a very good accuracy. Moreover, training the network on a set of realizations with different parameters than the test realizations, but which are nevertheless in the same physical phase, can also result in a network which can extract a reasonable entanglement entropy for the test realization. Thus, it is proposed that one train an artificial neural network on a system for which both an easily measured quantity and the entanglement may be measured or numerically calculated, then apply the network to infer the entanglement

entropy from the measured quantity.

Artificial neural networks have garnered a tsunami of publicity due to their application to a diverse set of tasks from speech recognition[26] to autonomous cars[27] and molecular synthesis design [28]. In quantum many-particle physics, there are several applications of machine learning [29]. Some are related to classifying different phases of matter [30–38], others to designing new materials [39–42], and also to representing the essence of many-particle states by neural network structures [43–45]. Very recently, machine learning was used to recognize order appearing in seemingly chaotic experimental data of cuprate Mott insulators in order to identify the physics behind the pseudo gap phenomenon [46]. Here, machine learning will be used for a different task, namely predicting one physical quantity based on the measurement of another, where there is no exact theoretical prescription to rely on. In this, we take advantage of the power of deep neural networks to learn from examples, i.e., after training the network on a set of realizations where both quantities (in this case primarily the number variance and entanglement entropy) are provided, the network is applied to other realizations for which it receives only one quantity and must infer the other. As we shall see, the training could be performed also on a non-interacting systems for which the calculation of the entanglement is much simpler than for the interacting target realizations.

One of the most popular quantification of entanglement is the entanglement entropy (EE), and its generalization, the Rényi entropy. These entropies measure the entanglement in a many-body system by dividing it into two regions A and B. For a system in a pure state  $|\Psi\rangle$ , the entanglement between regions A and B is related to the eigenvalues of the reduced density matrix of area A,  $\rho_A$  (or B,  $\rho_B$ ). Specifically,  $\rho_A$  is defined as:  $\rho_A = \text{Tr}_B |\Psi\rangle\langle\Psi|$ , where the degrees of freedom of region B are traced out. The eigenvalues  $\lambda_i^A$  of  $\rho_A$  are used to calculate the EE:

$$S_A = - \sum_i \lambda_i^A \ln \lambda_i^A, \quad (1)$$

Here, we illustrate these ideas for a 1D wire of length  $L = 700$  half-filled by spinless electrons with nearest-neighbor interactions and an on-site disordered potential. The Hamiltonian is given by:

$$H = \sum_{j=1}^L \epsilon_j \hat{c}_j^\dagger \hat{c}_j - t \sum_{j=1}^{L-1} (\hat{c}_j^\dagger \hat{c}_{j+1} + h.c.) \quad (2)$$

$$+ U \sum_{j=1}^{L-1} (\hat{c}_j^\dagger \hat{c}_j - \frac{1}{2})(\hat{c}_{j+1}^\dagger \hat{c}_{j+1} - \frac{1}{2}),$$

where  $\hat{c}_j^\dagger$  is the creation operator for a spinless electron at site  $j$ , and  $t = 1$  is the hopping matrix element. Since

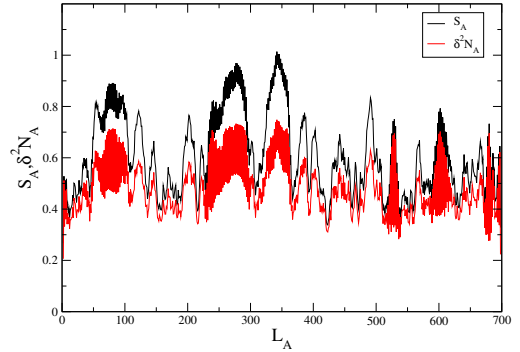


FIG. 1: The entanglement entropy,  $S_A$ , and the variance in number of particles,  $\delta^2 N_A$  for a single typical realization of disorder as function of the size of region A,  $L_A$ . These quantities show strong non-monotonic dependence on  $L_A$ , but nevertheless, there is a strong correspondence between them.

we want to test the case which the simple connection between number variance and EE is expected to fail, strong interaction ( $U = 2.4$ ) and weak disorder (where  $\epsilon_j$ , the on-site energy, is drawn from a uniform distribution of width 0.7, corresponding to a localization length,  $\xi \sim 14$ ) [47] were chosen for the targets. The eigenvalues,  $\lambda_i$ , for different sizes of region A between  $3 < L_A < L - 3$ , as well as the probability  $p_i(N_A^i)$  of measuring a specific number of particles  $N_A^i$  in the region, was calculated for 700 realizations of disorder using DMRG [48–51], with a block size of 392 and two sweeps through the system.

The EE,  $S_A$ , and the variance in number of particles, and  $\delta^2 N_A$ , are calculated using  $\lambda_i$ ,  $N_A^i$ , and  $p_i(N_A^i)$ . A detailed description of the computational method can be found in Ref. [47] and references therein.

In Fig. 1, the entanglement entropy  $S_A$ , and the number variance,  $\delta^2 N_A = \langle N_A^2 \rangle - \langle N_A \rangle^2$ , for a typical realization of disorder are presented. It is obvious that the two quantities fluctuate as a function of the size  $L_A$  of region A, and that there are sections for which there are strong even-odd fluctuation while other segments are rather smooth. Nevertheless, both quantities have a strong correlation between them. The simplest assumption would be a linear relation, which as we shall see, works reasonably well for the smooth regions, but fails for the strongly fluctuating one. Therefore, it looks plausible that by using machine learning which will identify the features of the region in the vicinity of  $L_A$  which may enable the network to determine  $S_A$  from  $\delta^2 N_A$ .

A rather simple neural network structure will be used in order to achieve this goal. Three main network structures were tested for this study, and as described in the supplementary material the network illustrated in Fig. 2 was chosen. Thus, here a convolutional neural network (CNN), similar to the ones used in speech recognition

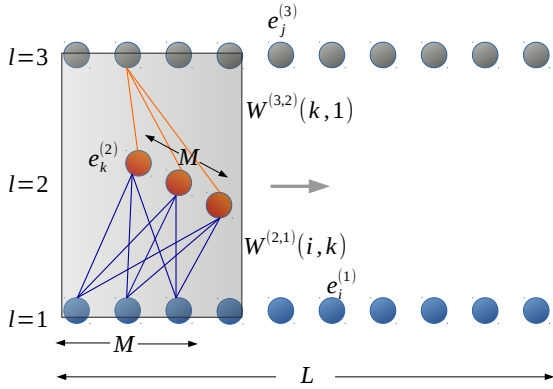


FIG. 2: The neural network which showed the best performance for reproducing the entanglement entropy,  $S_A$ , from the number variance  $\delta^2 N_A$  (labeled network C in the supplementary material). The lower (input) layer of neurons are the  $L$  values of  $\delta^2 N_A$  for a given realization and size of area  $A$ ,  $L_A$ , denoted by  $e^{(1)}$ , and the top layer are the output values of the entanglement entropy  $S_A$ , denoted by  $e^{(3)}$ . This network is a convolutional neural network where the hidden layer is composed of  $M$  input neurons termed  $e^{(2)}$ , each of them connected to  $M$  input neurons in the vicinity of output neuron  $L_A$ . The same weights  $W^{1,2}$  and  $W^{2,3}$  are used for all output neurons.

and image processing is used [26]. The basic unit is a neuron  $e_j^{(l)}$ , where  $l$  is the layer number ( $l = 1$  the input layer,  $l = 2$  hidden layer, and  $l = 3$  output layer). Each  $e_j^{(l)}$  can attain in principal any value. The size of the input layer is  $L$ , the size of the hidden layer is  $M$ , and the size of the output layer is  $L - M$ . There are two convolutional weight matrices connecting between consecutive layers  $W^{l,l+1}$ , where  $W^{1,2}$  is a  $M \times M$  matrix, and  $W^{2,3}$  is a  $M \times 1$  matrix. The matrices do not depend on the position of the output neuron  $j$ . Initially the matrices have random values between 0 and 0.1, while  $e_{L_A}^{(1)} = \delta^2 N_A(L_A)$  is the input layer. The higher layers are calculated by

$$\begin{aligned} e_k^{(2)} &= f \left( \sum_{i=k-M/2, k+M/2} W^{(1,2)}(i, k) e_i^{(1)} \right), \\ e_j^{(3)} &= f \left( \sum_{k=1, M} W^{(2,3)}(k, 1) e_k^{(2)} \right). \end{aligned} \quad (3)$$

where  $f(x)$  is a non-linear differentiable function, which here is taken as the Fermi function,  $f(x) = (1 + \exp(-x))^{-1}$ . As can be seen from the summation indices in Eq. (3), both layers are shifted according to the output neuron.

After generating the output, one should update the weights  $W^{(l,l+1)}$  according to the discrepancy between the output  $e_{L_A}^{(3)}$  and the entanglement entropy  $S_A(L_A)$ . Defining an error function,  $q = \sum_{L_A=1, L} (e_{L_A}^{(3)} -$

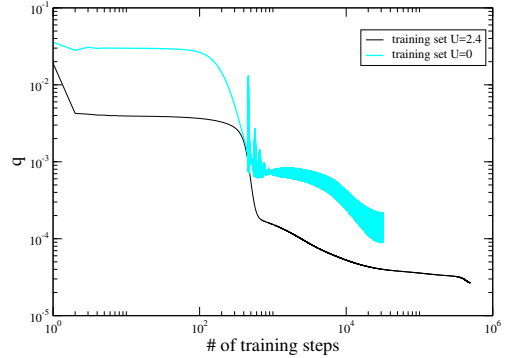


FIG. 3: The development of the error in the computed entanglement entropy  $q$  as functions of the number of training steps, measured for an ensemble of 200 realizations not included in the training set (test set), for the number variance,  $\delta^2 N_A$  as an input. Two different cases are shown: (black) A training set of 500 realizations with the same interaction parameter ( $U = 2.4$ , network C); (cyan) A training set of 300 non-interacting realizations ( $U = 0$ , network D).

$S_A(L_A))^2/L$ , the goal of the deep learning algorithm is to minimize  $q$  by adjusting the weights.

The backpropagation algorithm is used. Essentially a partial differentiation of  $q$  as a function of each weight is performed, and the weights are updated accordingly. Specifically,

$$\delta_j^{(l)} = \begin{cases} (e_j^{(l)} - S_A(j)) e_j^{(l)} (1 - e_j^{(l)}) & l = 3 \\ \sum_i \delta_i^{(l+1)} W^{(l,l+1)}(j, i) e_j^{(l)} (1 - e_j^{(l)}) & l = 2, \end{cases} \quad (4)$$

and the weights are updated accordingly:

$$\Delta W^{(l,l+1)}(i, j) = -\eta e_i^{(l+1)} \delta_j^{(l+1)}. \quad (5)$$

$\Delta W$  is summed over all realizations in the learning set and for different locations of the relevant weight  $W$  in the network. After completing the sweep, one updates the weights. The procedure continues until the desired accuracy  $q$  is obtained or until a preset number of training steps is reached. As a test of the ability of the network to predict the entanglement entropy for realizations on which it was not trained,  $q$  is calculated also for a set of different realizations of disorder, but no update of  $W$  is performed for those realizations.

In Fig. 3, the error,  $q$ , in the computed entanglement entropy as a function of the number of training steps is shown for the test set (realizations not included in the training). The value of the number variance,  $\delta^2 N_A$ , is used in order to generate the entanglement entropy  $S_A(L_A)$  as an output. The network show an initial plateau in  $q$ , followed by a decrease of  $q$ , i.e., the network has “learned” to produce a better correspondence between the observable and  $S_A(L_A)$ . It is interesting

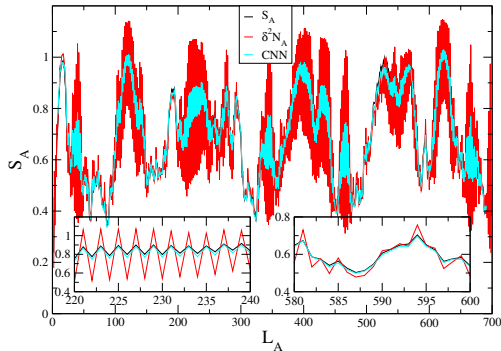


FIG. 4: The correspondence between the value of the entanglement entropy calculated directly by DMRG and by the deep CNN for a typical realization in the test set. The simplest assumption ( $S_A(L_A) \propto \delta^2 N_A(L_A)$ ) is indicated by the red curve. It is clear that the CNN gives an almost perfect fit. Left inset: Zoom into an area with strong even-odd fluctuations. Right inset: A region with weaker even-odd fluctuations.

to note that there is an initial short period (around  $10^3$  training steps) where a steep improvement in the error occurs, i.e., a period of accelerated learning. This period is followed by periods of slower decrease sometimes punctuated by additional accelerated learning periods. Examining closely a typical realization of disorder from the test set (Fig. 4), for the number variance as an input, the superiority of the results obtained by the CNN compared to a simple assumption  $S_A(L_A) \propto \delta^2 N_A(L_A)$  is self evident. It is very impressive that CNN can identify regions with enhanced even-odd fluctuations in  $\delta^2 N_A(L_A)$  and regions with more moderate fluctuations and respond accordingly.

Nevertheless, a questions remains: If the CNN works so well (as is evident from Fig. 4) what is the factor limiting the  $q$  value? The answer lies in some rare regions appearing in a few realizations of disorder for which the network fails to reproduce the EE. Such a rare region is presented in Fig. 5. One can see that the CNN results fits quite well the value of  $S_A$  anywhere except for  $150 < L_A < 250$ . Such behavior has been seen for about five samples out of the 200 in the test set. In all cases, the regions for which network fails are regions with anomalously high values of  $S_A$ , in the ballpark of the values expected for a clean system. Such rare regions, which exhibit metal-like behavior within an insulating phase, have been identified in a previous study [47]. These “microemulsion” metallic regions may be connected to the rare thermalizing inclusions postulated to drive the Griffiths phase close to the many-body localization transition [52, 53], to phase separation in two-dimensional systems [54], and to rare occurrences of enhancement of the per-

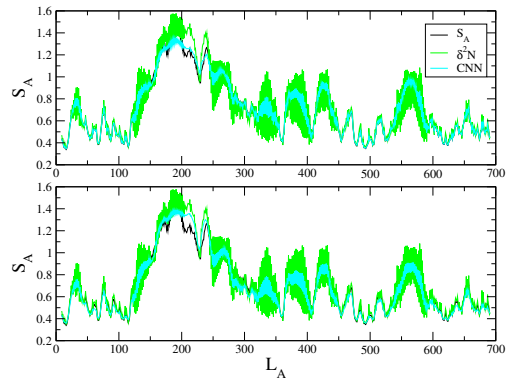


FIG. 5: (Top) The correspondence between the value of the entanglement entropy calculated directly by DMRG (black) and by CNN (cyan) for a rare realization in the test set. The variance is indicated in green. It can be seen that even for this rare realization the network does a decent job except for the region between sites 150 and 250. (Bottom) The same realization where the CNN was trained on a non-interacting ( $U = 0$ ) training set. Although the overall fit is not as good as in the case above, it is surprisingly decent.

sistent current in disordered interacting systems [55].

The fact that the CNN network learns almost perfectly to calculate  $S_A$  from  $\delta^2 N_A$  in the insulating phase and fails for the metallic like microemulsion is very interesting, and may lead one to argue that during the training the CNN has “learned” the features of the insulating phase. On the other hand, it can not infer the entanglement entropy of regions governed by different physics, i.e., the rare metallic regions. Thus, we have a computational procedure to calculate the entanglement entropy from the number variance which was created by supervised learning of a deep CNN, which seems to capture the physics of the majority phase of the system for the given parameters, but can not reproduce the entanglement for the rare regions belonging to a different phase.

Nonetheless, one remains with the problem that one must supply a training set for which both the observable and the entanglement entropy is known. For numerical studies where a direct calculation of the entanglement entropy might be computational expensive, but still doable, training such a network may show clear advantages. Success in extracting the entanglement from an observable for a numerical model also provides motivation to try to develop a theory connecting these quantities and may furnish clues towards its structure.

The question remains of how to train a system when the entanglement entropy is not known. One solution recently proposed is to try to extract the wavefunction out of the measurement of an observable(s), and use the wavefunction to extract the EE [56]. This is a promising method, but at the moment limited to small systems (of order of 20 sites). A different strategy for extracting the

entanglement is to train the CNN on a set corresponding to a system for which it is easier to obtain the entanglement and then apply it to the system we are interested in. As an example we tried training the CNN on a set of 300 samples for which  $W = 0.7$  and  $U = 0$  (non-interacting), and then test them on the 200 samples of the previous test set of the interacting system ( $w = 0.7, U = 2.4$ ). Since interactions here do not change the phase of the system (it remains an Anderson insulator), this might be expected to work. Nevertheless, using network C, although giving a better fit to the  $S_A$  than the proportionality to  $\delta^2 N_A$ , leaves much to be desired. Inserting an additional processing layer (see supplementary material, network D), which actually worsens somewhat the fit to a test set with the same parameters improves the fit to the interacting case. Network D results for the error are shown in Fig. 3, while the fit for the same realization which exhibits the rare region is shown on the bottom part of Fig. 5. For network D over training appears after  $\sim 310^4$  training steps. Thus, if the system can be reasonably represented by a numerically solvable model which can capture its main physical features, a situation common for cold-atom and for some solid-state systems, one could train the CNN using the calculation of the observable and entanglement entropy and then apply the network to the experimentally measured observable in order to extract the entanglement measure.

In conclusion, here it was shown that by using supervised machine learning it is possible to extract the entanglement between two regions of a disordered interacting many-particle system, a quantity which is very difficult to measure directly, by measuring more accessible observables. By training a neural network on several hundred realizations of disorder for which the entanglement as well as other observables are computed, it is then possible to apply the network on a new realization, for which the network has not been trained, and predict accurately the entanglement. It would be very useful to expand this method to higher dimensions.

- 
- [1] L. Amico, R. Fazio, A. Osterloh, and A. Vedral, Entanglement in many-body systems, *Rev. Mod. Phys.* **80**, 517 (2008).
- [2] R. Horodecki, P. Horodecki, M. Horodecki, and K. Horodecki, Quantum entanglement, *Rev. Mod. Phys.* **81**, 865 (2009).
- [3] J. I. Latorre, and A. Riera, A short review on entanglement in quantum spin systems, *J. Phys. A: Math. Theor.* **42** 504002 (2009).
- [4] I. Affleck, N. Lalorencie, and E. S. Sorensen, Entanglement entropy in quantum impurity systems and systems with boundaries, *J. Phys. A: Math. Theor.* **42** 504009 (2009).
- [5] J. Eisert, M. Cramer, and M. B. Plenio, Area laws for the entanglement entropy, *Rev. Mod. Phys.* **82**, 277 (2010).
- [6] A. Aspect, Bell's inequality test: more ideal than ever, *Nature* **398**, 189(1999).
- [7] M. A. Nielsen and I. L. Chuang, *Quantum Computation and Quantum Information* (Cambridge Univ. Press, 2010).
- [8] R. Berkovits, Entanglement Entropy in a One-Dimensional Disordered Interacting System: The Role of Localization, *Phys. Rev. Lett.* **108**, 176803 (2012).
- [9] J. H. Bardarson, F. Pollmann, and J. E. Moore, Unbounded Growth of Entanglement in Models of Many-Body Localization, *Phys. Rev. Lett.* **109**, 017202 (2012).
- [10] A. Zhao, R.-L. Chu, and S.-Q. Shen, Finite-size scaling of entanglement entropy at the Anderson transition with interactions, *Phys. Rev. B* **87**, 205140 (2013).
- [11] R. Berkovits, Entanglement Properties and Quantum Phases for a Fermionic Disordered One-Dimensional Wire with Attractive Interactions, *Phys. Rev. Lett.* **115**, 206401 (2015).
- [12] A. Kitaev and J. Preskill, Topological Entanglement Entropy, *Phys. Rev. Lett.* **96**, 110404 (2006).
- [13] M. Levin and X.-G. Wen, Detecting Topological Order in a Ground State Wave Function, *Phys. Rev. Lett.* **96**, 110405 (2006).
- [14] H.-C. Jiang, Z. Wang, and L. Balents, *Nature Phys.* **8**, 902 (2012).
- [15] P. Zanardi, C. Zalka, and L. Faoro, Entangling power of quantum evolutions, *Phys. Rev. A* **62**, 030301(R) (2000).
- [16] P. Horodecki and A. Ekert, Method for Direct Detection of Quantum Entanglement, *Phys. Rev. Lett.* **89**, 127902 (2002).
- [17] D. A. Abanin and E. Demler, Measuring Entanglement Entropy of a Generic Many-Body System with a Quantum Switch, *Phys. Rev. Lett.* **109**, 020504 (2012).
- [18] A. J. Daley, H. Pichler, J. Schachenmayer, and P. Zoller, Measuring Entanglement Growth in Quench Dynamics of Bosons in an Optical Lattice, *Phys. Rev. Lett.* **109**, 020505 (2012).
- [19] R. Islam, R. Ma, P. M. Preiss, M. E. Tai, A. Lukin, M. Rispoli, and M. Greiner, Measuring entanglement entropy in a quantum many-body system, *Nature* **528**, 77 (2015).
- [20] A. M. Kaufman, M. E. Tai, A. Lukin, M. Rispoli, R. Schittko, P. M. Preiss, and M. Greiner, Quantum thermalization through entanglement in an isolated many-body system, *Science* **353**, 794 (2016).
- [21] A. Elben, B. Vermersch, M. Dalmonte, J. I. Cirac, and P. Zoller, Rényi Entropies from Random Quenches in Atomic Hubbard and Spin Models, *Phys. Rev. Lett.* **120**, 050406 (2018).
- [22] I. Klich and L. Levitov, Quantum Noise as an Entanglement Meter, *Phys. Rev. Lett.* **102**, 100502 (2009).
- [23] H. F. Song, S. Rachel, C. Flindt, I. Klich, N. Laflorencie, K. and Le Hur, Bipartite fluctuations as a probe of many-body entanglement, *Phys. Rev. B* **85**, 035409 (2012).
- [24] I.S. Burmistrov, K.S. Tikhonov, I.V. Gornyi, A.D. and Mirlin, Entanglement entropy and particle number cumulants of disordered fermions, *Ann. of Phys.* **383**, 140 (2017).
- [25] B. Hsu, E. Grosfeld, and E. Fradkin, Quantum noise and entanglement generated by a local quantum quench, *Phys. Rev. B* **80**, 235412 (2009).
- [26] Y. Zhang, M. Pezeshki, P. Brakel, S. Zhang, C. Laurent, Y. Bengio, and A. Courville, Towards End-to-End Speech Recognition with Deep Convolutional Neural Networks,

- arXiv:1701.02720.
- [27] Y. Tian, K. Pei, S. Jana, and B. Ray, DeepTest: Automated Testing of Deep-Neural-Network-driven Autonomous Cars, arXiv:1708.08559.
- [28] M. H. S. Segler, M. Preuss, and M. P. Waller, Planning chemical syntheses with deep neural networks and symbolic AI, *Nature* **555**, 604 (2018).
- [29] L. Zdeborova, Machine learning: New tool in the box, *Nature Phys.* **13**, 420 (2017).
- [30] P. Broecker, J. Carrasquilla, R. G. Melko, and S. Trebst, Machine learning quantum phases of matter beyond the fermion sign problem, *Sci. Rep.* **7**, 8823 (2017),
- [31] K. Chng, J. Carrasquilla, R. G. Melko, and E. Khatami, Machine Learning Phases of Strongly Correlated Fermions, *Phys. Rev. X* **7**, 031038 (2017).
- [32] Y. Zhang and E.-A. Kim, Quantum Loop Topography for Machine Learning, *Phys. Rev. Lett.* **118**, 216401 (2017).
- [33] D.-L. Deng, X. Li, and S. Das Sarma, Machine Learning Topological States, *Phys. Rev. B* **96**, 195145 (2017).
- [34] T. Ohtsuki and T. Ohtsuki, Deep Learning the Quantum Phase Transitions in Random Two-Dimensional Electron Systems, *J. Phys. Soc. Jpn.* **85**, 123706 (2016).
- [35] J. Carrasquilla and R. G. Melko, Machine learning phases of matter, *Nature Phys.* **13**, 431 (2017).
- [36] E. P. L. van Nieuwenburg, Y.-H. Liu, S. D. and Huber, Learning phase transitions by confusion, *Nature Phys.* **13**, 435 (2017).
- [37] W. Hu, R. R. P. Singh, and R. T. Scalettar, Discovering Phases, Phase Transitions and Crossovers through Unsupervised Machine Learning: A critical examination, *Phys. Rev. E* **95**, 062122 (2017).
- [38] F. Schindler, N. Regnault, and T. Neupert, Probing many-body localization with neural networks, *Phys. Rev. B* **95**, 245134 (2017).
- [39] A. G. Kusne, T. Gao, A. Mehta, L. Ke, M. C. Nguyen, K.-M. Ho, V. Antropov, C.-Z. Wang, M. J. Kramer, C. Long, and I. Takeuchi, On-the-fly machine-learning for high-throughput experiments: search for rare-earth-free permanent magnets, *Sci. Rep.* **4**, 6367 (2014).
- [40] L. M. Ghiringhelli, J. Vybiral, S. V., Levchenko, C. Draxl, and M. Scheffler, Big Data of Materials Science: Critical Role of the Descriptor, *Phys. Rev. Lett.* **114**, 105503 (2015).
- [41] S. V. Kalinin, B. G. Sumpter, and R. K. Archibald, Bigdeepsmart data in imaging for guiding materials design, *Nature Mater.* **14**, 973 (2015).
- [42] L. Li, T. E. Baker, S. R. White, and K. Burke, Pure density functional for strong correlation and the thermodynamic limit from machine learning, *Phys. Rev. B* **94**, 245129 (2016).
- [43] G. Torlai, and R. G. Melko, Learning thermodynamics with Boltzmann machines, *Phys. Rev. B* **94**, 165134 (2016).
- [44] G. Carleo and M. Troyer, *Science* **355**, 602 (2017).
- [45] D.-L. Deng, X. Li, and S. Das Sarma, Quantum Entanglement in Neural Network States, *Phys. Rev. X* **7**, 021021 (2017).
- [46] Yi Zhang, A. Mesaros, K. Fujita, S. D. Edkins, M. H. Hamidian, K. Ch'ng, H. Eisaki, S. Uchida, J. C. Samus Davis, E. Khatami and Eun-Ah Kim, Using Machine Learning for Scientific Discovery in Electronic Quantum Matter Visualization Experiments, arXiv:1808.00479.
- [47] R. Berkovits, Low eigenvalues of the entanglement Hamiltonian, localization length, and rare regions in one-dimensional disordered interacting systems, *Phys. Rev. B* **97**, 115408 (2018).
- [48] S. R. White, Density matrix formulation for quantum renormalization groups, *Phys. Rev. Lett.* **69**, 2863 (1992).
- [49] S. R. White, Density-matrix algorithms for quantum renormalization groups, *Phys. Rev. B* **48**, 10345 (1993).
- [50] U. Schollwöck, The density-matrix renormalization group, *Rev. Mod. Phys.* **77**, 259 (2005).
- [51] K. A. Hallberg, *Adv. Phys.* **55**, 477 (2006).
- [52] S. Gopalakrishnan, M. Muller, V. Khemani, M. Knap, E. Demler, and D. A. Huse, Low-frequency conductivity in many-body localized systems, *Phys. Rev. B* **92**, 104202 (2015).
- [53] L. Zhang, B. Zhao, T. Devakul, and D. A. Huse, Many-body localization phase transition: A simplified strong-randomness approximate renormalization group, *Phys. Rev. B* **93**, 224201 (2016).
- [54] B. Spivak and S. A. Kivelson, Phases intermediate between a two-dimensional electron liquid and Wigner crystal, *Phys. Rev. B* **70**, 155114 (2004); R. Jamei, S. Kivelson, and B. Spivak, Universal Aspects of Coulomb-Frustrated Phase Separation, *Phys. Rev. Lett.* **94**, 056805 (2005).
- [55] P. Schmitteckert, R. A. Jalabert, D. Weinmann, and J.-L. Pichard, From the Fermi Glass towards the Mott Insulator in One Dimension: Delocalization and Strongly Enhanced Persistent Currents, *Phys. Rev. Lett.* **81**, 2308 (1998).
- [56] G. Torlai, G. Mazzola, J. Carrasquilla, M. Troyer, R. Melko and G. Carleo, Neural-network quantum state tomography, *Nature Physics*, **14**, 447 (2018).